Residual stress relaxation induced by shot peening in different materials after quasi-static loading

J. Hoffmeister[1], V. Schulze[1]

1 Institute for applied materials, Karlsruhe Institute of Technology (KIT), Germany

Abstract

Shot peening is often used to improve the fatigue life of cyclic loaded components. Therefore it is very important to know the changes of the residual stress state due to quasi-static loading. The objective of this work was to describe the changes of the residual stress state of different materials caused by shot peening induced by quasi-static loading. Therefore different shot peened specimens were loaded isothermally up to a specific tensile load. After the different loadings the residual stresses at the surface and for special loadings the residual stress depth distributions were determined experimentally by using X-ray diffraction. With an already existing model, based on the surface-core-model, the deformation behaviour of the surface could be deduced from the results of the quasi-static experiments. The model was adapted so that it is possible to predict the residual stress relaxation according to the residual stress and the full width at half maximum depth distribution and a stress-strain curve of hole drilled specimen. The remaining material in the gauge length of the hollow drilled specimen is much more affected by the mechanical surface treatment. So rather the hardening or the softening of the material could be measured and integrated in the modelling.

Keywords: Inconel® 718, IN718, AISI 4140, residual stresses, stability

Introduction

Shot peening can significantly increase the fatigue life of cyclic loaded components. The improvement of the properties can be attributed to near-surface residual stresses and work hardening. Because of mechanical relaxation of the residual stresses the mechanical properties can be reduced. For the design of cyclic loaded components it is therefore very important to know the dependence of the stress relaxation on the mechanical loading. To describe the mechanical residual stress relaxation analytical and FE-models can be used. Both procedures have their difficulties. The analytical models must be adapted by costly experimental results. The FE-Models normally base on complex material models and the surface state after the mechanical surface treatment must be generated with complex process models. In this paper the mechanical macro residual stress relaxation is described by a model which bases on the procedure of [1, 2]. The model was adapted so that the residual stress relaxation under quasi static loading can be modelled with only one tensile test and the initial residual stress and full width of half maximum (FWHM) depth distribution.

Methods

The investigations were carried out on age hardened Inconel® 718 (IN718) and quenched and tempered AISI 4140 round specimens. The outer diameters of the samples were 7 mm. The cylindrical surfaces of the samples were shot peened. The material state, Almen intensity and testing temperatures of different investigated material states or rather materials are summarized in Table 1. In order to find out the change of the quasi-static residual stresses, interrupted tensile tests were performed. In addition to the interrupted tensile tests specimen were mechanically drilled and afterwards the drill hole was enlarged to a diameter of 6.6 mm by wire electro discharge machining. This ensures that the remaining material is not additionally work hardened. With these hollowed specimen tensile tests were performed at the testing temperature. The surface residual stresses were measured before and after the mechanical loading by X-ray diffraction. The measurement conditions and basis of calculation for the residual stresses are listed for the different investigated materials. For the residual stress evaluation the $\sin^2\psi$-method was used. For selected mechanical loadings the complete depth distributions of residual stresses were measured by alternating electro polishing and measuring steps. Because the removed area was small, the stress relaxation could be ignored.

Table 1: Material, material states and testing conditions

	IN718 (0.1 mmA)	IN718 (0.25 mmA)	AISI 4140 (0.21 mmA)
heat treatment	solution annealing: 955 – 985°C for 1h ageing treatment: 720°C for 8h and 620°C for 8h		Quenched and tempered for 2 h at 450°C
Almen intensity	0.1 mmA	0.25 mmA	0.21 mmA
testing temperature	TT < 750°C	TT < 750°C	RT (room temperature)

Table 2: measurement conditions and basis of calculation for the residual stresses

	IN718	AISI 4140
Interference line	{311}	{211}
Radiation	Mn-Kα	Cr-Kα
Youngs Moduls of the interference line $E^{\{\}}$	200 GPa	219.911 GPA
Possion ratio of the interference line $\nu^{\{\}}$	0.32	0.28
Stress free diffraction angle $2\theta_0$	151°	156.394°

Experimental Results

The initial material states were characterised. The residual stress and FWHM depth distribution of the two materials and corresponding material states are shown in Figure 1.

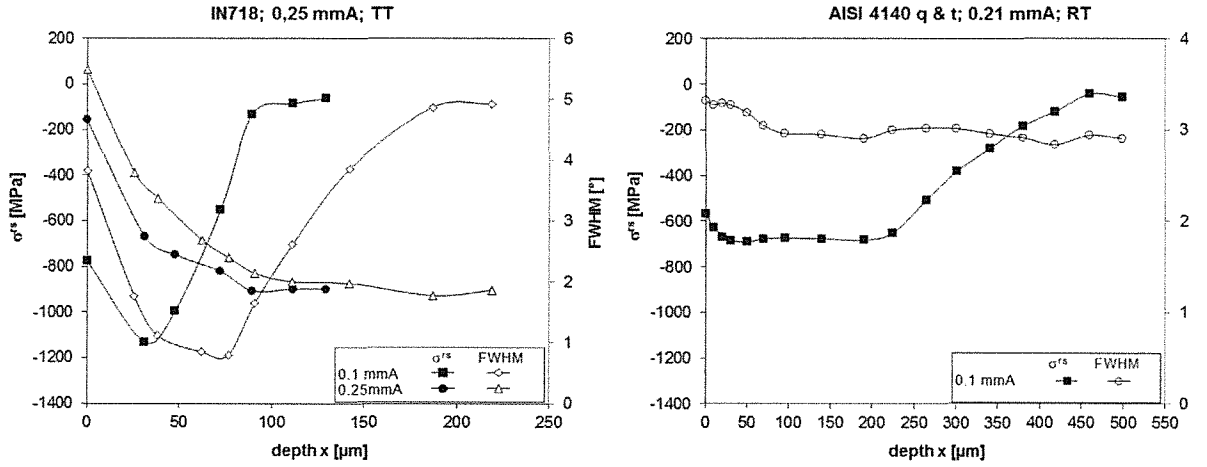

Figure 1: Initial residual stress and FWHM depth distributions for the two material states of IN718 (on the left after a thermal treatment on TT) and quenched and tempered AISI 4140 (on the right)

For the material IN718 the depth distribution are illustrated after a thermal relaxation (Figure 1 left). The two material states of IN718 both show a residual stress depth distribution with maximum compressive residual stresses beneath the surface. The material state which was peened with the higher Almen intensity shows the higher penetration depth. The penetration depth of the FWHM is also higher for the higher Almen intensity. The FWHM depth distributions have a clear trend. Both material states have the highest value of FWHM at the surface and the FWHM decrease continually until the FWHM value of the untreated material is achieved. The residual stresses and FWHM for the quenched and tempered AISI 4140 are illustrated in Figure 1 on the right. The compressive residual stresses also have their maximum value beneath the surface but there is a plateau of the residual stress values. In comparison to the IN718 the penetration depth is higher and the FHWM show no clear tendency. This is typical for this material and material state [3]. The residual stresses after different quasi-static loads are shown in Figure 2 on the left for the different material states of IN718 and on the right for the steel AISI 4140. All materials show the same behaviour: The surface residual stresses are

nearly constant until the total strain achieves the elastic limit. After this, the compressive residual stresses first build up slightly and decrease afterwards. For the two material states of IN718 tensile residual stresses are built up. The steel AISI 4140 shows no zero crossing of surface residual stresses and the surface residual stresses keep nearly constant at a value of σ^{rs} = -300 MPa. The stress-strain curves for the different materials and material states are also presented in Figure 2. In this figure also the material behavior of an untreated material state is shown. Both material states of IN718 achieve higher stresses than the untreated material. The stress-strain-curves of both material states of IN718 show a hardening of the material. For the state of 0.1 mmA the elastic limit was measured higher than the elastic limit of the untreated state. The elastic limit of the 0.25 mmA state has a lower elastic limit than the untreated state. The steel AISI 4140 shows a lower elastic limit, but the stresses run completely under the stress-strain-curve of the untreated material. So the material seems to be softened.

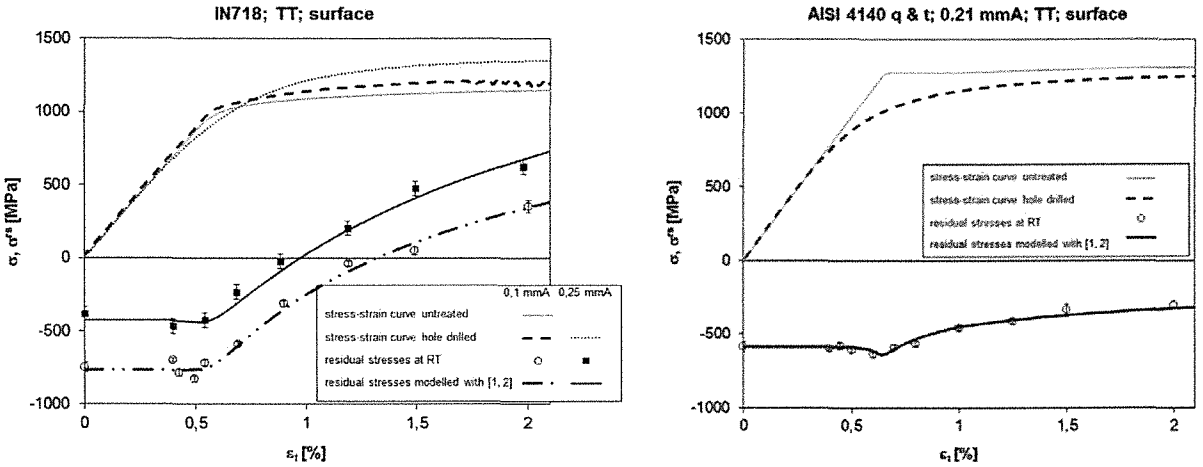

Figure 2: Measured stress-strain curve of the untreated, the hole drilled specimen as well as the measured and modelled [1, 2] surface residual stresses after the mechanical loading for the two material states of IN718 (left) and the quenched and tempered steel AISI 41440 (right)

The measured depth distributions of the residual stresses (Figure 4 and 5) show the same behavior at and near the surface. For depths larger than the depth of the maximum compressive residual stresses, the residual stresses do not cross the zero line. It can also be seen that the depths of the maximum and the zero-crossing of the residual stresses are almost constant.

Discussion

The result can be modelled as already presented in [1, 2]. The model bases on the surface-core-model [4-6], the deformation behaviour of the surface can be deduced from the results of the quasi-static experiments. The model was expanded to a multi-layer model so that the complete residual stress distribution after quasi-static loading can be described. The result of this modelling for the surface can be seen in Figure 2. There is a good correlation for the two material states of IN718 and the modelling can be applied for the steel AISI 4140. The model can reproduce the buildup of the compressive residual stresses. But the modelling is very costly, especially for the IN718 tests at elevated temperatures. The specimens must be heated up stepwise, mechanical loaded and the residual stress must be measured. So it would be fine to model the quasi static residual stress relaxation with an easier way. In the model of [1, 2] it was possible to calculate the stress-strain curve of a hole drilled specimen, beside the calculation of residual stresses, if the hardening is known as a function of the depth. So it should also be possible to calculate the residual stress relaxation if the hardening as a function of the depth and the stress-strain curve of hole drilled specimen are known. In [1, 2] the distribution of FHWM was directly correlated with the technical elastic limit at 1 % plastic stain $R_{p,1\%}(x)$.

$$R_{p,1\%}(x) = \left[\frac{x - x_0}{x_0}\right]^4 \cdot (R_{p,1\%,surface} - R_{p,1\%,core}) + R_{p,1\%,core} \quad for\ x < x_0$$
$$R_{p,1\%}(x) = R_{p,1\%,core} \quad for\ x \geq x_0 \tag{1}$$

$R_{p,1\%}(x)$ is the technical elastic limit at 1 % plastic strain as a function of the depth x, $R_{p,1\%,surface}$ and $R_{p,1\%,core}$ are the technical elastic limit at 1 % plastic strain for the surface and the core and x_0 is the depth of zero crossing of the residual stress. This equation was deduced from the depth distribution of the full width at half maximum (FWHM), which is used as an indicator for work hardening. Additional it was accepted that the distribution of the strain hardening coefficient distribution of K(x) of the Ramberg-Osgood-approach [7] has secondary effects on the calculation of residual stress. So a linear correlation was taken:

$$K(x) = \left|\left[\frac{x - x_0}{x_0}\right]\right| \cdot (K_{surface} - K_{core}) + K_{core} \quad for\ x < x_0$$
$$K(x) = K_{core} \quad for\ x \geq x_0 \tag{2}$$

K(x) is the hardening coefficient as a function of the depth x, $K_{surface}$ and K_{core} are the hardening coefficient for the surface and the core and x_0 is the depth of zero crossing of the residual stresses. The strain hardening exponent as function of depth *n(x)* can be calculated by converting of the Ramberg-Osgood approach [4]:

$$n(x) = \frac{\log((R_{p,1\%}(x)/K(x))}{\log(0.01)} = \frac{\log(K(x)) - \log(R_{p,1\%}(x))}{2} \tag{3}$$

The whole hardening of shot-peened specimens can be described with the equations (1) and the Ramberg-Osgood-approach. The parameters $R_{p,1\%,core}$, K_{core} and x_0 can be deduced from the experiments. The parameters $R_{p,1\%,surface}$ and $K_{surface}$ must be determined. Therefore the hollow drilled specimen is subdivided into 20 layers. The work hardening behaviour corresponding to coefficient K(x) and exponent n(x), compare Eq. (1 - 3)) is related to each layer corresponding to the mean depth of the layer. Because the residual stresses relocate during the hole drilling process, a residual stress free specimen is assumed. So it is possible to calculate the stress σ_n as a function of the applied total strain ε_t for every layer. After averaging the stresses σ_n of every layer the same total strain ε_t results in the stress–strain curve of the hollow drilled specimen. By changing the $R_{p,1\%,surface}$ and $K_{surface}$ the calculated stress-strain curve and measured stress–strain curve can be approximated. For the approximation of the stress-strain respectively $R_{p,1\%,surface}$ and $K_{surface}$ curve a least square algorithm was used. So it is also possible to calculate a stress strain-curve for the surface by using $R_{p,1\%,surface}$ and $K_{surface}$ and shifting to the residual strain which can be calculated by Hooke's law and the residual stresses at the surface before mechanical loading. Assuming a linear–elastic unloading process the residual stress relaxation for the surface residual stresses after a quasi-static mechanical loading can be determined (compare [1, 2]). The result of this proceeding can be seen in Figure 3. The beginning of the residual stress relaxation can be predicted very well. Furthermore the change of sign as well as the range of resulting residual stresses can be predicted with this method in dependency of the mechanical loading. Details like the build-up of compressive residual stress cannot be predicted. Residual stress relaxation of the model is in all case more pronounced than in the experiment, so the model gives a conservative estimate. With the calculated distribution of work hardening behaviour it is according to [1, 2] also possible to calculate the residual stress depth distribution after a quasi-static mechanical loading. The results are shown in Figure 4 (left 0.1 mmA and right 0.25 mmA) for IN718 and in Figure 5 for the steel AISI 4140.

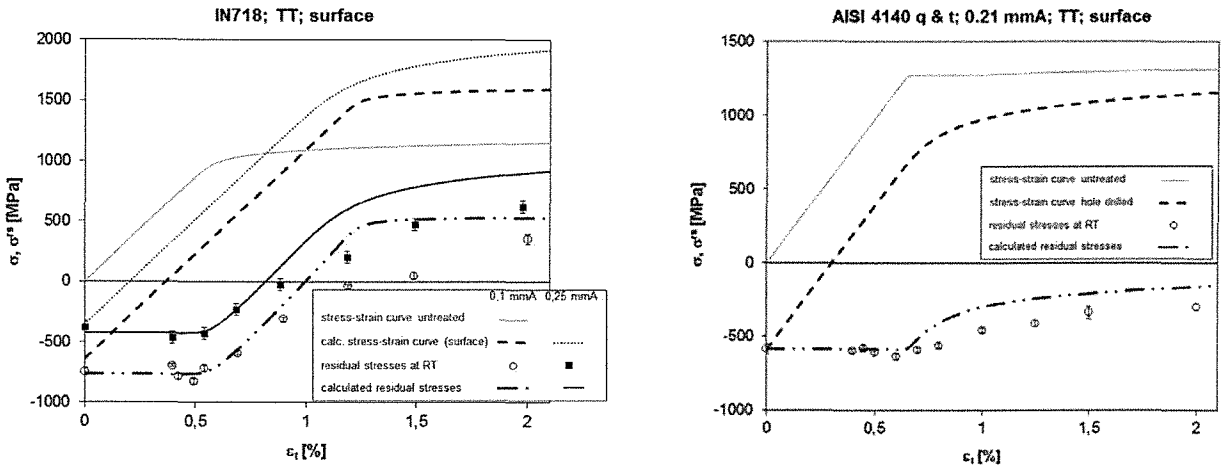

Figure 3: Measured stress-strain curve of the untreated material, with the data of the hole drilled and shot peened specimen calculated stress-strain curve at surface and testing temperature as well as the measured and calculated surface residual stress at room temperature. On the left the two different material states of IN718 and on the right the data for the quenched and tempered steel AISI 4140 are shown

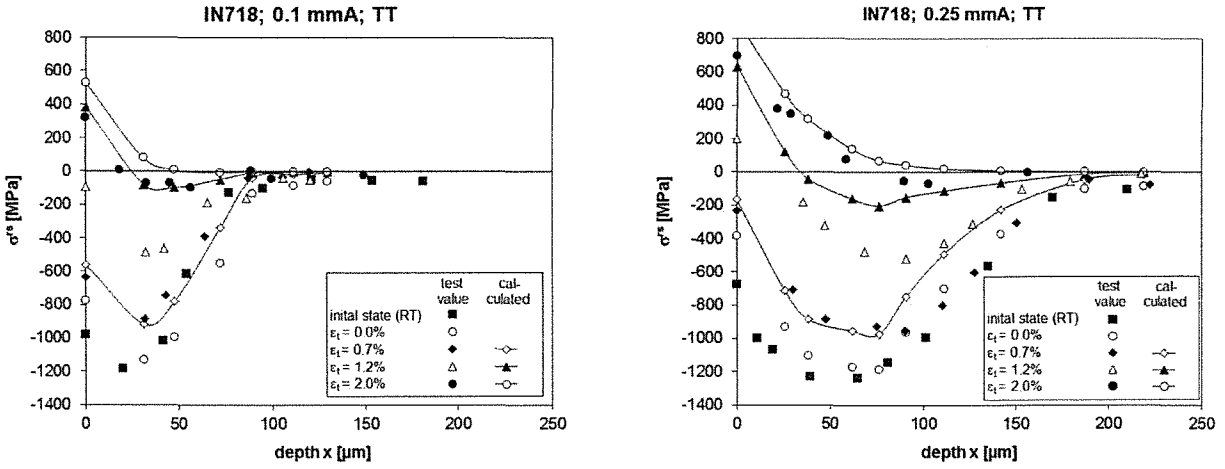

Figure 4: Measured and calculated residual stress depth distributions after different quasi-static mechanical loading and different shot peening states
0.1 mmA (left) and 0.25 mmA (right) for IN718

The measured and the calculated residual stress depth distributions correlate in principle. But the model overestimates the residuals stress relaxation as already determined for the surface residual stress relaxation (compare Figure 3). The calculated residual stress depth distributions for the steel AISI 4140 show a greater discrepancy from the measured values. This can be explained with the material state. For this ageing condition the hardening state depth distribution cannot be correlated directly with the FWHM depth distribution. So there the correct basis for modelling is not available here. In order to get better results with this modelling the hardening depth distribution should be known well, the hole diameter should adapted to the hardening depth distribution and in the best case the residual stress distribution of the hole drilled specimen should be known.

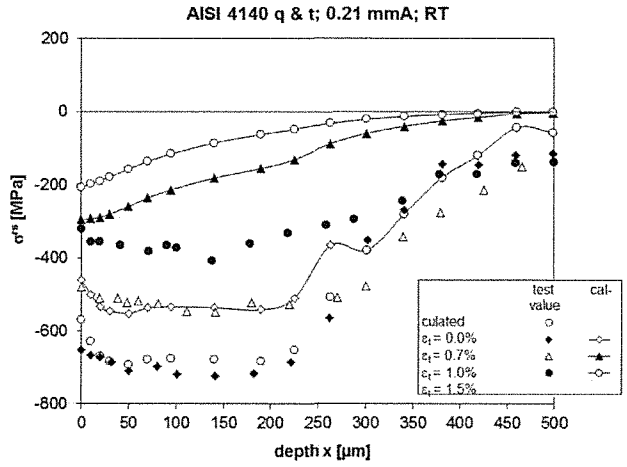

Figure 5: Measured and calculated residual stress depth distributions after different quasi-static mechanical loading for the quenched and tempered steel AISI 4140 (0.21 mmA)

Conclusion

The residual stress relaxation of shot peened IN718 and AISI 4140 after an isothermal quasi-static loading was modelled based on the measured initial residual stress and FWHM depth distributions and stress-strain curve of shot peened and hole drilled specimens. With this modelling residual stress relaxation can be predicted. It was possible to predict the begin of the residual stress relaxation. Furthermore changes of sign as well as the range of resulting residual stresses can be predicted. The original model of [1, 2] which was the basic for the modelling show better results for both materials, but the model is more costly. The prediction of the residual stress depth distribution after a mechanical loading was only possible for IN718. For steel AISI 4140 there was no good arrangement. This could be explained with the material state. For this ageing condition the hardening state depth distribution cannot correlate directly with the FWHM depth distribution. So there is not the correct basis for modelling. But for material respectively material states which have a clearly tendency of hardening state depth distribution it is possible to calculate the residual stress depth distribution after quasi static mechanical loading with the presented model.

References

[1] Hoffmeister J, Schulze V., Hessert R., Koenig G.: *Residual Stress Relaxation Induced by Shot Peening in Inconel718 Under Quasistatic and Cyclic Loading*. In: Champaigne J, editor. ICSP11; 2011. p. 225–230

[2] Hoffmeister J, Schulze V., Hessert R., Koenig G.: *Residual stresses under quasi-static and cyclic loading in shot peened Inconel 718*, International Journal of Materials Research - Zeitschrift für Metallkunde * Band 103 (2012) Heft 1, Seite 66-72

[3] V.Schulze: *Modern Mechanical Surface Treatment*, Wiley VCH, Weinheim, 2006

[4] O. Vöhringer, in: V. Hauk E. Macherauch (eds.): *Abbau von Eigenspannungen, Eigenspannungen, DGM-Informationsgesellschaft*, Oberursel, 1983, pp. 49-83

[5] O. Vöhringer, In: A. Niku-Lari (eds.): *Relaxation of residual stresses by annealing or mechanical treatment*, Advances in surface treatment; International Guidebook on Residual Stresses, Pergamon, New York, 1987, pp. 367-395

[6] T. Hirsch: *Zum Einfluß des Kugelstrahlens auf die Biegeschwingfestigkeit von Titan- und Aluminiumbasislegierungen*, Dissertation, Universität Karlsruhe (TH), 1983

[7] W. Ramberg, W. R. Osgood, NASA (non Center Specific): *Description of stress-strain curves by three parameters*, NACA Technical Note 902. (1943).